Crystal Structure of Poly(7-heptalactone)

Malafronte, Anna; Scoti, Miriam; Caputo, Maria; Li, Bo; O'Reilly, Rachel; Dove, Andrew; Müller, Alejandro; De Rosa, Claudio

DOI:
10.1021/acs.macromol.3c00710

Document Version
Publisher's PDF, also known as Version of record

Citation for published version (Harvard):
Malafronte, A, Scoti, M, Caputo, M, Li, B, O'Reilly, R, Dove, A, Müller, A & De Rosa, C 2023, 'Crystal Structure of Poly(7-heptalactone)', *Macromolecules*, vol. 56, no. 11, pp. 4153-4162. https://doi.org/10.1021/acs.macromol.3c00710

Macromolecules

pubs.acs.org/Macromolecules Article

Crystal Structure of Poly(7-heptalactone)

Anna Malafronte,* Miriam Scoti, Maria Rosaria Caputo, Bo Li, Rachel K. O' Reilly, Andrew P. Dove, Alejandro J. Müller, and Claudio De Rosa*

Cite This: *Macromolecules* 2023, 56, 4153−4162 Read Online

ACCESS | Metrics & More | Article Recommendations | Supporting Information

ABSTRACT: The crystal structure of poly(7-heptalactone) (PHL) is presented. PHL has been synthesized by a combination of ring-opening polymerization of η-heptalactone and reversible addition−fragmentation chain transfer polymerization using diphenyl phosphate as catalyst. The noncommercial available η-heptalactone monomer has been prepared by oxidation of cycloheptanone. The crystal structure of PHL has been determined by analysis of the X-ray powder diffraction profiles and of the electron diffraction patterns of single crystals and calculations of lattice energy. The structure has been refined with the Rietveld full-profile refinement. Chains in *trans* planar conformation are packed in an orthorhombic unit cell with axes a = 7.37 Å, b = 5.05 Å, and c = 10.07 Å according to the space group symmetry $P2_1$.

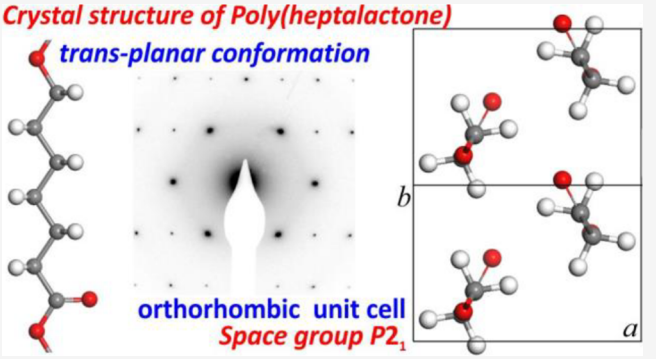

INTRODUCTION

At present the research on plastics is focused on searching for solutions to minimize the environmental impact.[1−4] Attention is devoted to developing materials from renewable resources, as an alternative to petroleum-derived polymers, and to studying polymers able to biodegrade in a reasonably short time without forming toxic and/or harmful products.[4] Aliphatic polyesters are the ideal candidates for these aims, due to their hydrolytic degradability (that occurs by hydrolysis of the ester bonds) and, for most of which, the ease of finding monomers from renewable resources for their synthesis.[5] In addition, many aliphatic polyesters are biocompatible, which makes them also interesting in the biomedical field.[6,7]

Since the properties (such as biodegradation rate) of aliphatic polyesters depend on numerous factors including structure, molecular mass, crystallinity, and morphology, a complete understanding of the relationships among crystalline structure and properties is a crucial point for the future design of biodegradable polymers with well-defined and desired physical properties.

The crystal structures of linear aliphatic polyesters, −(−O−$(CH_2)_m$−CO−)$_n$−, have been extensively studied.[8−24] All linear aliphatic polyesters with an even or odd number of methylene units in the backbone (m) adopt an all-*trans* planar or close to the *trans* planar conformation.[8,9,11,15−19,22−24] The number of methylene groups (m) plays an important role in determining the chain symmetry of linear aliphatic polyesters. When m is odd, the molecular chain in a nearly *trans* planar conformation presents a 2/1 helical symmetry. When m is even, the chain in a *trans* planar conformation has the carbonyl groups on the same side of the chain backbone, and, therefore, presents only a mirror symmetry plane, which corresponds to the plane of the *trans* planar chain.

Almost all linear aliphatic polyesters crystallize in orthorhombic unit cells with values of a and b axes comprised in between 6.0−7.7 and 4.9−5.2 Å, respectively,[8,9,11,15,16,18,22,23] and of the c axis that depends on the number of methylene groups. These values of a and b axes are similar to those of the orthorhombic form of polyethylene (PE) (a = 7.40 Å and b = 4.93 Å).[25] Only for poly(15-pentadecalactone) (m = 14), a monoclinic unit cell, but still with a pseudo-orthorhombic packing, has been proposed.[24]

Among the different aliphatic polyesters, poly(ε-caprolactone) (PCL) (m = 5) has been extensively studied both in terms of crystallization behavior[17−20] and properties, being biocompatible and biodegradable and used for many different applications, such as tissue engineering and drug delivery systems.[26,27] PCL is usually synthesized by ring-opening polymerization (ROP) of ε-caprolactone. An alternative novel material is poly(7-heptalactone) (PHL), −(−O−$(CH_2)_6$−CO−)$_n$−, an aliphatic polyester derived from η-heptalactone that presents an even number of methylene units in the backbone m = 6. The presence of one more carbon atom than PCL could affect the crystallization behavior and the crystal structure, even though properties such as processability

Received: April 14, 2023
Revised: May 11, 2023
Published: June 2, 2023

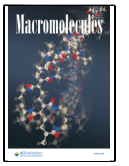

and physical properties are expected to be similar to those of PCL.

Although PHL is potentially an interesting crystalline polyester, it has been largely understudied compared to other aliphatic polyesters, in particular PCL, due to the noncommercial availability of the η-heptalactone monomer. In fact, few studies of the polymerization of η-heptalactone to PHL have appeared in the literature,[28,29] one of which concerns the enzymatic polymerization catalyzed by lipase,[29] and one paper reports the ROP of η-heptalactone employing metal-catalyzed coordinative-insertion polymerization.[28] In particular, although the ROP of lactones of different ring sizes promoted by metal-based catalysts has been extensively studied,[30−39] the ROP of the eight-membered lactone, η-heptalactone, has been reported only recently employing a discrete lanthanum compound, $La[N(SiMe_3)_2]_3$, and salen-ligated yttrium and lanthanum complexes as catalysts to produce high molecular mass PHL.[28] In the same report, the yttrium and lanthanum catalysts have been employed for the stereoselective copolymerization of η-heptalactone with eight-membered cyclic diester (diolide) to produce block copolymers of PHL with poly(3-hydroxybutyrate).[28] In our recent previous report,[40] PHL of low polydispersity of the molecular mass has been synthesized by ROP of η-heptalactone combined with reversible addition−fragmentation chain transfer (RAFT) polymerization using diphenyl phosphate (DPP) as catalyst. The η-heptalactone monomer has been prepared by oxidation of cycloheptanone according to the procedure described in the literature.[29]

In this paper, we report for the first time the determination of the crystal structure of PHL by wide-angle X-ray diffraction of powder samples and electron diffraction (ED) of single crystals coupled to conformational and packing energy calculations. The analyzed sample of PHL has been prepared as in our previous paper,[40] resulting in low polydispersity and suitable molecular mass to successfully obtain single crystals and a high degree of crystallinity in the bulk.

EXPERIMENTAL SECTION

PHL was synthesized as described in our previous report,[40] by a combination of ROP of η-heptalactone (Scheme 1) and RAFT polymerization, using DPP as catalyst and 4-cyano-4-(((ethylthio)-carbonothioyl)thio) pentanoic acid as an initiator and chain transfer agent [see the Supporting Information (SI)], according to the procedure also reported in ref 41, used for the synthesis of PCL and different block copolymers based on PCL. DPP was selected as catalyst due to its superior ability to give polylactones with narrow dispersities.[42] The monomer η-heptalactone has been prepared by Baeyer−Villiger oxidation of cycloheptanone (see the SI).[29]

Scheme 1. Scheme of the Preparation of PHL by ROP of η-Heptalactone Catalyzed by DPP

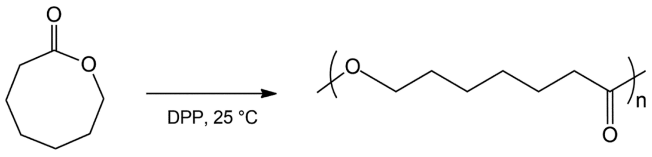

The PHL sample was characterized by ^{1}H and ^{13}C NMR and size exclusion chromatography (SEC). The nuclear magnetic resonance (NMR) spectra and the SEC curve are reported in the SI (Figures S3−S5), whereas the ^{13}C NMR spectrum is also reported in Figure 1. The observed resonances assigned to the different carbon atoms of the CH_2 groups and to the carbonyl carbon atom in the ^{13}C NMR spectrum and to the hydrogen atoms in the ^{1}H NMR spectrum (Figure S3) confirm the molecular structure of the synthesized PHL.[28,40] The average molecular mass and distribution of molecular masses are reported in Table 1. The sample shows narrow distribution of molecular masses with $M_w/M_n \approx 1.15$ according to the synthetic strategy.

The crystallization properties of PHL have been analyzed by X-ray diffraction and differential scanning calorimetry (DSC). Details of the crystallization from the melt by compression molding, and the characterization by X-ray diffraction and DSC are described in the SI.

Single crystals were obtained by crystallization from solution of PHL in 1-hexanol at 50 °C (see the SI). Single crystals were imaged in the transmission electron microscope (TEM) in bright field (BF) mode and ED patterns of single crystals were acquired.

Structural modeling, energy calculations and diffraction simulations were performed by using Accelrys BIOVIA Materials Studio (MS) software package (see the SI). Calculations of the conformational and packing energies were carried out by using the consistent-valence forcefield (CVFF).[43] No interactions for distances longer than 20 Å were taken into account.

The crystal structure was refined by Rietveld powder diffraction refinement based on standard nonlinear least-square algorithms.[44,45] The agreement between the calculated and the experimental diffraction profiles was evaluated from the figures of merit of the best fit, defined as the weighted profile residual factor R_{wp} and the profile residual factor R_p, as defined in the SI.

RESULTS AND DISCUSSION

The X-ray powder diffraction profiles of the as-prepared sample of PHL and DSC curves recorded during the heating of the as-prepared sample, successive cooling, and heating of the melt-crystallized sample are reported in Figures 2 and 3, respectively. The melting and crystallization temperatures of the sample, obtained from DSC data of Figure 3, are reported in Table 1.

The diffraction profile of the as-prepared sample of PHL is characterized by two main diffraction peaks of high intensity at 2θ = 21.4° and 24.2° (Figure 2A) and other minor peaks at higher values of the Bragg angle (Figure 2A'). The diffraction profile indicates that the sample shows high degree of crystallinity of nearly 50%.

The as-prepared sample melts at ≈64 °C and crystallizes from the melt by cooling at 10 °C/min at nearly 50 °C (Figure 3, Table 1). The diffraction profile of the melt-crystallized compression molded sample of PHL (Figure 4) is essentially identical to the profile of the as-prepared sample (Figure 2) with a similar degree of crystallinity, indicating that PHL crystallizes from the polymerization solution and from the melt in the same crystalline form.

All diffraction peaks visible in the X-ray diffraction profile of the as-prepared sample (Figure 2) are reported in Table 2.

Single crystals of PHL have been crystallized from 1-hexanol solution as described in the SI. The TEM BF image of the crystals is reported in Figure 5A. Hexagonal-shaped flat single crystals have been obtained, most of which are multilayered. This morphology has been observed in the literature for other polyesters, such as poly(11-undecalactone) (PUDL)[9] and PCL.[46] Single crystals with various thicknesses have been observed (Figure 5A) and ED patterns with numerous spots (Figure 5B) have been obtained from single-lamellar crystals and from the single-lamellar zone at the border of all multilayered crystals.

The ED pattern of single crystals of PHL of Figure 5B contains 12 independent diffraction spots mirrored in the four

https://doi.org/10.1021/acs.macromol.3c00710
Macromolecules 2023, 56, 4153−4162

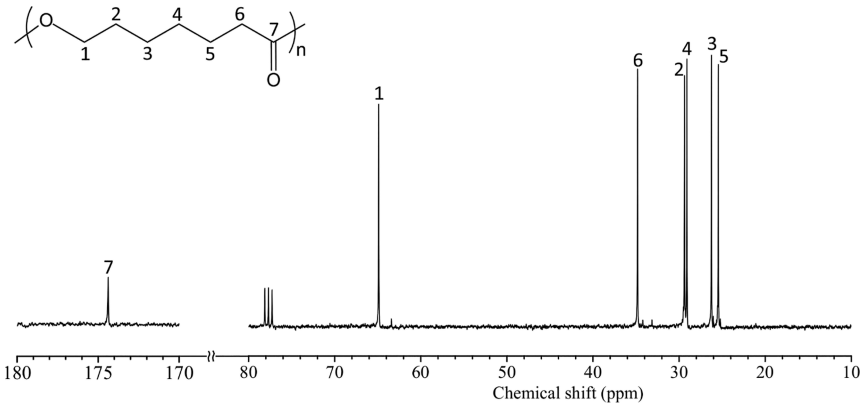

Figure 1. ^{13}C NMR spectrum of the synthesized sample of PHL in $CDCl_3$ solution. The assignment of the observed resonances to carbon atoms shown in the scheme is indicated.

Table 1. Average Molecular Masses (M_n and M_w), Polydispersity ($Đ_M$), Melting Temperature of the As-Prepared (T_m^I) and Melt-Crystallized (T_m^{II}) Samples and Crystallization Temperature (T_c) of PHL

sample	M_n (kDa)[a]	M_w (kDa)[a]	$Đ_M$[a]	T_m^I (°C)[b]	T_c (°C)[b]	T_m^{II} (°C)[b]
PHL	16.6	19.6	1.15	63.6	49.7	61.8

[a]From SEC. [b]From the DSC curves of Figure 3 at scanning rate of 10 °C/min.

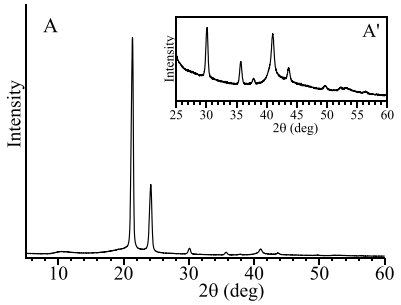

Figure 2. X-ray powder diffraction profile of the as-prepared sample of PHL. The profile at high values of 2θ is shown in an enlarged scale in A′.

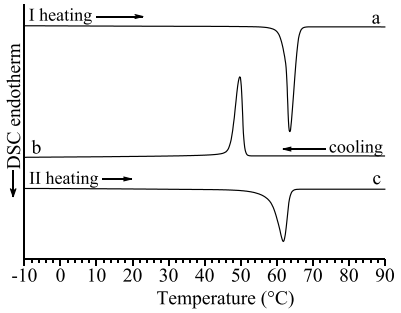

Figure 3. DSC curves recorded at 10 °C/min during first heating of the as-prepared sample (a), cooling from the melt (b), and successive heating (c) of the melt-crystallized sample of PHL.

quadrants and corresponds to the a^*b^* plane of the reciprocal lattice defined by the two orthogonal axes a^* and b^*. All the observed ED spots are equatorial reflections and can be indexed in terms of a rectangular reciprocal lattice with parameters $a^* = 1.359\ nm^{-1}$, $b^* = 1.984\ nm^{-1}$, and $\gamma^* = 90°$,

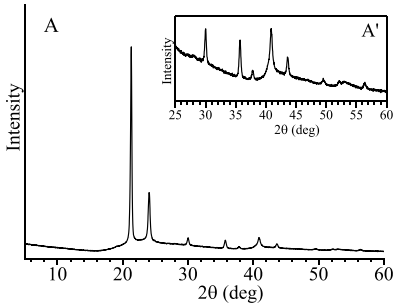

Figure 4. X-ray powder diffraction profile of the melt-crystallized sample of PHL. The profile at high values of 2θ is shown in an enlarged scale in A′.

Table 2. Diffraction Angles ($2\theta_o$), Bragg Spacings (d_o), and Intensities (I_o) of the Reflections Observed in the X-ray Powder Diffraction Profile of the As-Prepared Sample of PHL (Figure 2) and in the ED Pattern of Single Crystals of PHL (Figure 5B)

X-ray powder diffraction profile (Figure 2)				electron diffraction (Figure 5B)		
$2\theta_o$ (deg)	d_o (nm)	I_o	hkl[a]	d_o (nm)	I_o[b]	hkl[a]
10.46	0.846	140	001			
19.20	0.462	2	011			
21.36	0.416	2440	110	0.417	vvs	110
24.17	0.368	870	200	0.368	vvs	200
30.10	0.297	74	210	0.297	s	210
35.72	0.251	33	020	0.252	vvs	020
37.82	0.238	8	120	0.239	m	120
41.00	0.220	120	310	0.220	vs	310
43.65	0.207	19	220	0.208	m	220
49.67	0.183	8	400	0.184	m	400
52.27	0.175	3	320	0.176	w	320
53.13	0.172	5	410	0.173	vw	410
56.36	0.163	4	130	0.164	w	130
				0.151	vw	420

[a]All reflections are indexed based on an orthorhombic unit cell with axes $a = 7.37$ Å, $b = 5.05$ Å, and $c = 10.07$ Å. [b]vvs = very very strong; vs = very strong; s = strong; m = medium; w = weak; and vw = very weak.

corresponding to a direct planar unit cell with parameters $a = 7.36$ Å, $b = 5.04$ Å, and $\gamma = 90°$. Along both the two a^* and b^* axes, systematic absences of reflections occur at every h and k

https://doi.org/10.1021/acs.macromol.3c00710
Macromolecules 2023, 56, 4153−4162

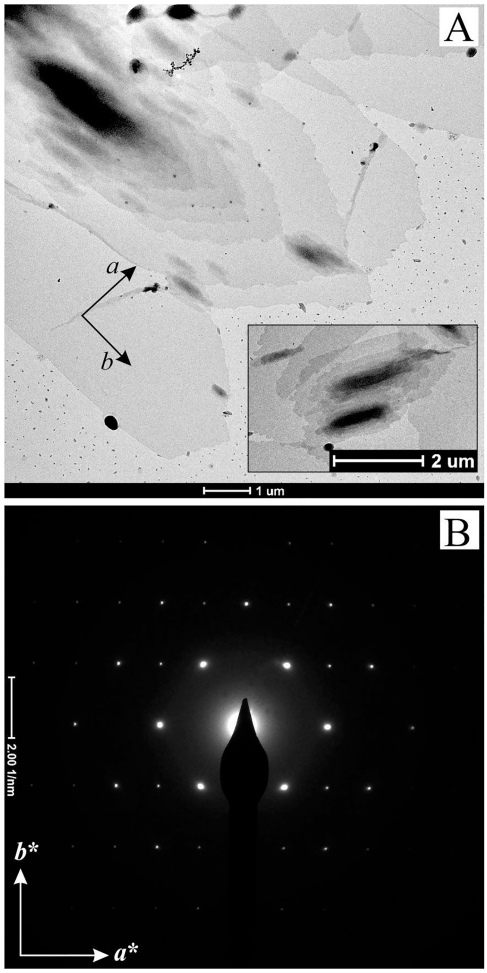

Figure 5. BF TEM image (A) and ED pattern (B) of PHL single crystals. The directions of the *a* and *b* axes of the unit cell and of *a** and *b** of the reciprocal lattice are indicated.

odd and only the *h*00 and 0*k*0 reflections with *h* and *k* even, respectively, are observed. The Bragg spacing *d* of all reflections observed in the ED pattern of Figure 5 are reported in Table 2, in comparison with those of the diffraction peaks observed in the X-ray powder diffraction profile of Figure 2. The comparison shows that the *d*-spacings of all reflections observed in the ED pattern and in the powder diffraction profile are similar, indicating that the as-prepared and melt-crystallized samples and the single crystals are in the same crystalline form.

There is a close similarity between the ED patterns of PHL and other aliphatic polyesters, $-(-O-(CH_2)_m-CO-)_n-$, such as poly(*β*-propiolactone) (PPL) (*m* = 2),[11] poly(*δ*-valerolactone) (PVL) (*m* = 4),[16] PCL (*m* = 5),[17−20] PUDL (*m* = 10),[9] poly(12-dodecalactone) (PDDL) (*m* = 11),[23] poly(15-pentadecalactone) (PPDL) (*m* = 14)[24] and poly(16-hexadecalactone) (PHDL) (*m* = 15).[22] As previously mentioned, all linear aliphatic polyesters with an even or odd number of methylene units in the backbone (*m*) adopt a *trans* planar or close to all-*trans* planar conformation.[8,9,11,15−19,22−24] Based on these numerous previous well-established studies, an all-*trans* planar conformation of the chains of PHL has been assumed in this study. A low-energy chain model of PHL in *trans* planar conformation has been built assuming the geometry shown in Scheme 2 with bond lengths and bond angles taken from ref 9 (Table 3) and backbone torsion angles of 180°. The low-energy model of PHL is reported in Figure 6.

Scheme 2. Scheme of the Monomeric Unit of PHL with the Labeling of Carbon and Oxygen Atoms

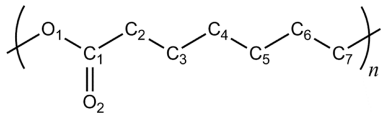

Table 3. Values of Bond Lengths and Bond angles[9] of the PHL Chain in the *Trans* Planar Conformation[a]

bond lengths (Å)	
O_1-C_1	1.35
$C_1=O_2$	1.23
C_1-C_2	1.51
C_n-C_{n+1} (n = 2−6)	1.54
C_7-O_1	1.48
bond angles (deg)	
$O_1-C_1=O_2$	125.0
$O_1-C_1-C_2$	114.0
$O_2=C_1-C_2$	121.0
$C_1-C_2-C_3$	113.0
$C_n-C_{n+1}-C_{n+2}$ (n = 2−5)	112.5
$C_6-C_7-O_1$	115.0
$C_7-O_1-C_1$	116.0

[a]Atoms are indicated according to labels shown in Scheme 2.

The chain period containing one monomeric unit results equal to *c* = 10.07 Å (Figure 6). As mentioned, since the number of methylene groups in the backbone is even, this conformation presents only a mirror symmetry plane, which corresponds to the plane of the *trans* planar chain. Since X-ray fiber diffraction patterns of PHL could not be obtained because of the low molecular mass that has prevented stretching the samples of PHL at a high degree of deformation to produce oriented fibers, we assume that the periodicity of the chain conformation of 10.07 Å of the model of Figure 6 corresponds to the *c* axis of the unit cell. The proposed orthorhombic unit cell with axes *a* = 7.36 Å, *b* = 5.04 Å, and *c* = 10.07 Å may host two chains of PHL in the *trans* planar conformation resulting in a crystalline density of 1.14 g/cc, which agrees with the values of crystalline density of similar polyesters.[9−24]

The packing of the chains of PHL in the *trans* planar conformation of Figure 6 in the orthorhombic unit cell with axes *a* = 7.36 Å and *b* = 5.04 Å (as determined by the ED pattern of Figure 5B) and *c* = 10.07 Å was analyzed assuming different possible space groups symmetry considering the systematic absences of *h*00 and 0*k*0 reflections with *h* and *k* odd and the condition that two chains are hosted in the unit cell. The lattice energy and the X-ray diffraction profile of the models of packing have been calculated to select the model that gives low lattice energy and the best agreement between the calculated and experimental X-ray powder diffraction profile and the ED pattern of Figures 2 and 5B, respectively. The best agreement has been obtained with a model characterized by a $P2_1$ space group (a monoclinic symmetry with unique axis *b*, full symmetry $P12_11$) and keeping the orthorhombic symmetry of the unit cell with *β* = 90°.

https://doi.org/10.1021/acs.macromol.3c00710
Macromolecules 2023, 56, 4153−4162

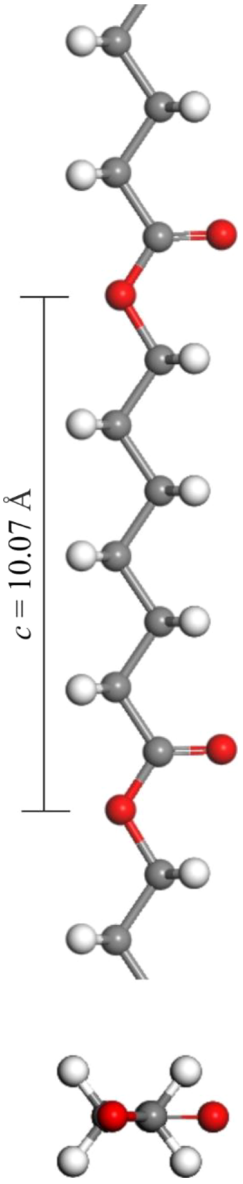

Figure 6. Model of the chain of PHL in the *trans* planar conformation with internal coordinates reported in Table 3, viewed along projections parallel and normal to the chain axis. The chain periodicity of 10.07 Å is indicated. Oxygen, carbon, and hydrogen atoms are represented in red, gray, and white, respectively.

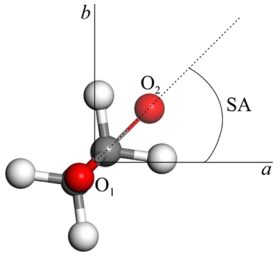

Figure 7. Definition of parameters variable in the calculation of the lattice energy and of the diffraction patterns: the setting angle (SA) is defined as the angle between the dashed line, which identifies the projection of the atom O_2 on the *ab* plane, and the *a* axis (positive for a counterclockwise rotation), whereas the height of the chain is defined as the *z*/*c* fractional coordinate of the atom O_1.

Calculations of the lattice energy and of the diffraction patterns were performed by changing the angle of rotation of the chain around the chain axis and the height of the chain along the *z* axis, while keeping fixed geometry and conformation of the chain (Table 3 and Figure 6). The angle of rotation around the chain axis (setting angle, SA) is defined as the angle between the plane of the backbone and the *a* axis, therefore the angle defined in Figure 7 by the position of the atom O_2 with respect to the *a* axis, whereas the variable height of the chain is defined as the *z*/*c* fractional coordinate of the atom O_1 (see Figure 7 and Scheme 2).

The chain of PHL in the *trans* planar conformation was placed in the unit cell with the centroid of the bond C_3-C_4 (Scheme 2) at the fractional coordinates *x*/*a* = 0.25 and *y*/*b* = 0.25. In this model, the unit cell hosts two polymer chains related by the 2_1 helical axis parallel to the *b* axis; therefore, the two chains have opposite orientations along the *c* axis.

Map of the lattice energy (*E*) as a function of the SA and *z*/*c* (defined in Figure 7) for a model of PHL chains in *trans* planar conformation of Figure 6 packed in the orthorhombic unit cell with axes *a* = 7.36 Å, *b* = 5.04 Å, and *c* = 10.07 Å according to the space group $P2_1$ is reported in Figure 8. The map is

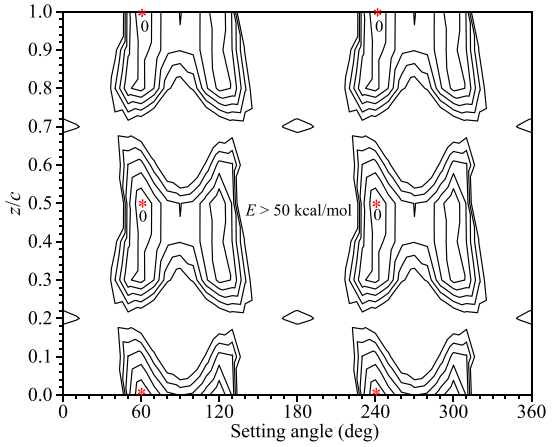

Figure 8. Map of the lattice energy (*E*) as a function of the setting angle (SA) and *z*/*c* (defined in Figure 7) for a model of packing of PHL chains in *trans* planar conformation (Figure 6) packed in the orthorhombic unit cell with axes *a* = 7.36 Å, *b* = 5.04 Å, and *c* = 10.07 Å, according to the space group $P2_1$. The centroid of the bond C_3-C_4 (see Scheme 2) is placed at fractional coordinates *x*/*a* = 0.25 and *y*/*b* = 0.25. The energy levels are drawn at intervals of 10 kcal/mol with respect to the absolute minimum of the map assumed as zero (indicated by asterisks).

periodic over SA = 180° and *z*/*c* = 0.5. Moreover, the map is nearly symmetric with respect to the SA of 90°. The absolute energy minimum (indicated with an asterisk in Figure 8) has been found for values of SA = 60° and *z*/*c* = 0. Due to the periodicity of the map over SA = 180° and *z*/*c* = 0.5, equivalent energy minima are present at SA = 60°, *z*/*c* = 0.5 and SA = 240°, *z*/*c* = 0 and 0.5. Moreover, due to the symmetry with respect to SA = 90°, nearly equivalent energy minima are present at SA = (90° ± 30°) and *z*/*c* = 0 and 0.5, and at SA = (270° ± 30°) and *z*/*c* = 0 and 0.5. Therefore, additional nearly equivalent energy minima are found at SA = 120° and 300°, *z*/*c* = 0 and 0.5.

The low-energy model of packing, corresponding to SA = 60° and *z*/*c* = 0 of Figure 8, has been refined with the Rietveld

https://doi.org/10.1021/acs.macromol.3c00710
Macromolecules 2023, 56, 4153−4162

powder diffraction full-profile refinement using the diffraction profile of Figure 2. In the refinement, the starting position of the polymer chain was chosen at the SA equal to 60° and the z/c fractional coordinate of the atom O_1 equal to zero, that is, at values corresponding to the absolute energy minimum of Figure 8.

In the fitting between the calculated and experimental diffraction profiles, the structural parameters changed and refined during the refinement procedure are the SA, the *xy* coordinate of the chain axis, defined by the fractional coordinates of the centroid of the bond C_3-C_4 (Scheme 2), initially positioned at $x/a = 0.25$ and $y/b = 0.25$, and its height along *z*. The *a* and *b* axes of the unit cell and the widths of the diffraction peaks, related to the sizes of crystallite, were also refined. A background polynomial (order 20) was used for fitting the experimental background (which includes the amorphous phase contribution) and the background coefficients were refined. Hydrogen atoms were considered in the simulation of the diffraction pattern and the calculation of agreement factors. Global anisotropic temperature factors in the *a*, *b*, and *c* crystallographic directions (B_x, B_y, and B_z) were assumed and the best agreement was obtained for values equal to $B_x = B_y = 8$ Å^2 and $B_z = 20$ Å^2.

The refinement produces a satisfactory fit of the calculated and experimental diffraction profiles, and the satisfactory agreement factors $R_{wp} = 12.0\%$ and $R_p = 8.8\%$ (see SI) were achieved. The obtained refined parameters are reported in Table 4. The final refined model of packing of PHL is reported

Table 4. Refined Parameters Obtained after the Rietveld Refinement Procedure of the PHL Crystal Structure in the Model of Figure 9[a]

lattice parameters	
a (Å)	7.3715 ± 0.0006
b (Å)	5.0510 ± 0.0004
parameters defining the chain position	
x/a	0.2415
y/b	0.2490
z/c	−0.0338
SA (deg)	62
crystallite sizes	
A (Å)	220 ± 2
B (Å)	330 ± 3
C (Å)	29 ± 1

[a] *a* and *b* axes of the orthorhombic unit cell, fractional coordinates (x/a and y/b) of the centroid of the bond C_3-C_4 (Scheme 2), fractional coordinate (z/c) of the atom O_1 (Scheme 2), setting angle (SA), and crystallite size broadening parameters (*A*, *B*, *C*).

in Figure 9. The proposed model has a low lattice energy as it corresponds to SA = 62° and $z/c = -0.0338$ (Table 4) very close to the absolute minimum of packing energy of Figure 8. The comparison between the X-ray powder diffraction profile calculated for the model of packing of Figure 9 and the experimental X-ray powder diffraction profile of Figure 2, shown in Figure 10, indicates that a good agreement has been obtained. The comparison between calculated diffraction angles ($2\theta_c$), *d*-spacings (d_c), and diffraction intensities (I_c) of *hkl* reflections for the model of Figure 9 and observed diffraction angles ($2\theta_o$), *d*-spacings (d_o), and intensities (I_o) determined from the diffraction profile of Figure 2 is reported in Table 5. The fractional coordinates of the atoms of the

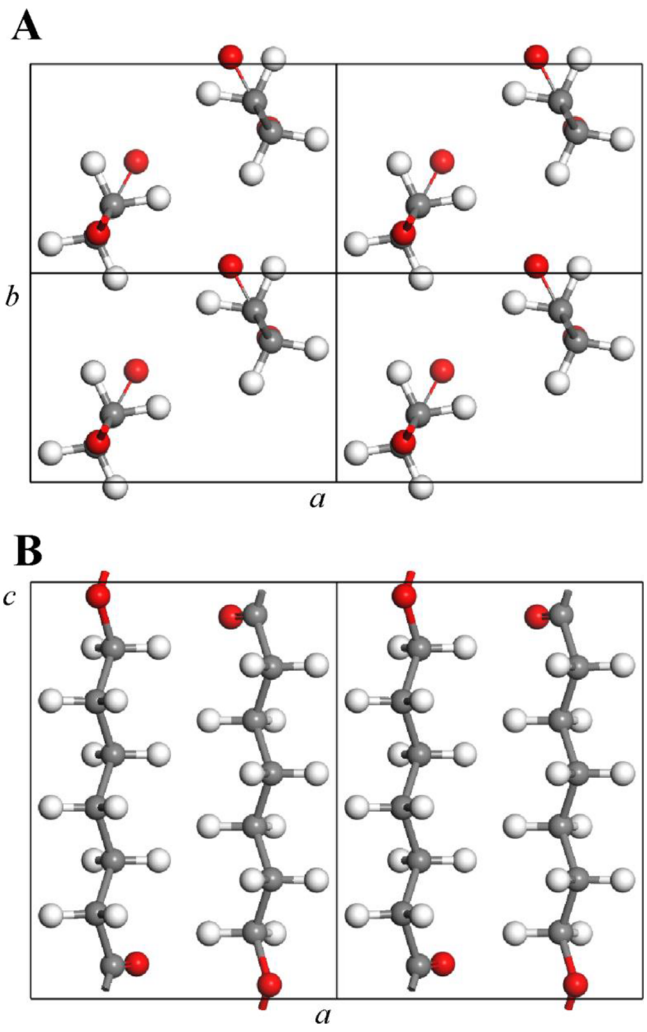

Figure 9. Model of the crystalline structure of PHL viewed in *ab* (A) and *ac* (B) projections. Chains in *trans* planar conformation are packed in an orthorhombic unit cell with axes $a = 7.37$ Å, $b = 5.05$ Å, and $c = 10.07$ Å, according to the space group $P2_1$ (unique axis *b*). Oxygen, carbon, and hydrogen atoms are represented in red, gray, and white, respectively.

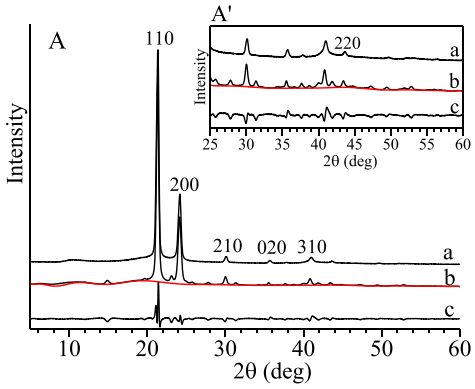

Figure 10. Comparison between the experimental diffraction profile of PHL of Figure 2 (curve a) and the diffraction profile calculated for the model of packing of Figure 9 (curve b). The red line is the background (including the amorphous phase contribution). Curve (c) is the difference profile. The 2θ region comprised between $2\theta = 25°$ and 60° is reported in an enlarged scale in A'. The *hkl* reflections that contribute most to the calculated diffraction intensities are indicated.

https://doi.org/10.1021/acs.macromol.3c00710
Macromolecules 2023, 56, 4153−4162

Table 5. Observed Diffraction Angles ($2\theta_o$), *d*-Spacings (d_o), and Intensities (I_o) of *hkl* Reflections Evaluated from the Experimental Diffraction Profile of PHL of Figure 2, and Calculated Diffraction Angles ($2\theta_c$), *d*-Spacings (d_c), and Intensities (I_c) of *hkl* Reflections for the Model of Packing of Figure 9 in the Orthorhombic Unit Cell with Axes a = 7.37 Å, b = 5.05 Å, c = 10.07 Å, and Space Group $P2_1$

hkl	$2\theta_o$ (deg)	$2\theta_c$ (deg)	d_o (nm)	d_c (nm)	I_o[a]	I_c[b]
001	10.46	8.78	0.846	1.007	16	24
100		12.00		0.737		1 → 25
101	-	14.90	-	0.595	-	7
002	-	17.62	-	0.503	-	2
011	19.20	19.66	0.462	0.451	0.2	1
110	21.36	21.32	0.416	0.417	284	230
102		21.38		0.416		3 → 233
111	24.17	23.10	0.368	0.385	101	7
200		24.14		0.368		102 → 110
012		24.98		0.356		2
201	-	25.74	-	0.349	-	3
112	-	27.80	-	0.321	-	3
103	-	29.24	-	0.305	-	0.6
210	30.10	30.01	0.297	0.298	9	9
202		30.05		0.297		2 → 11
211	-	31.33	-	0.286	-	3
013	-	32.02	-	0.279	-	0.5
113	-	34.31	-	0.261	-	0.9
212	-	35.02	-	0.256	-	0.7
020	35.72	35.54	0.251	0.252	4	3
203	-	36.20	-	0.248	-	0.5
120	37.82	37.65	0.238	0.239	1	1
301		37.68		0.239		0.4 → 2
104		37.77		0.238		0.5
121	-	38.73	-	0.232	-	0.9
014	41.00	40.03	0.220	0.225	14	4
310		40.84		0.221		9
122		41.85		0.216		0.7 → 16
311		41.86		0.216		0.7
114		41.94		0.215		2
220	43.65	43.43	0.207	0.2083	2	2
204		43.55		0.2078		1 → 3
312	-	44.80	-	0.202	-	0.7
214	-	47.29	-	0.192	-	1
400	49.67	49.46	0.183	0.184	1	1
024	-	51.25	-	0.178	-	0.4
320	52.27	51.92	0.175	0.176	0.3	0.7
124	53.13	52.84	0.172	0.173	0.6	1
410		52.88		0.173		0.4 → 1
130	56.36	56.02	0.163	0.164	0.5	0.4

[a]Scaled so that $\sum I_o = \sum I_c$. [b]Only reflections with a calculated intensity equal or higher than 0.4 are reported.

https://doi.org/10.1021/acs.macromol.3c00710
Macromolecules 2023, 56, 4153−4162

asymmetric unit of the model of the crystal structure of PHL of Figure 9 are reported in Table 6.

Table 6. Fractional Coordinates of the Carbon and Oxygen Atoms of the Asymmetric Unit of PHL in the Model of the Crystalline Structure of Figure 9 in the Orthorhombic Unit Cell with Axes a = 7.37 Å, b = 5.05 Å, c = 10.07 Å, and Space Group $P2_1$

atom	x/a	y/b	z/c
O_1	0.220	0.191	−0.034
O_2	0.346	0.532	0.084
C_1	0.267	0.318	0.079
C_2	0.214	0.174	0.204
C_3	0.269	0.324	0.332
C_4	0.214	0.174	0.459
C_5	0.269	0.324	0.586
C_6	0.214	0.175	0.713
C_7	0.269	0.324	0.840

The refined values of a and b lattice parameters (a = 7.372 and b = 5.051 Å, Table 4) are very close to the values determined from the ED pattern (a = 7.36 Å, b = 5.04 Å, Figure 5B). In the unit cell, the carbon atom of the carbonyl group of one chain is shifted along c by 0.159c with respect to the carbonyl group of the other antiparallel chain (Figure 9B). The arrangement of the PHL chains in the ab projection (Figure 9A) is quite similar to that of PE[25] and PCL,[17−20] and other linear aliphatic polyester of type $-(-O-(CH_2)_m-CO-)_n-$.[9,11,15,16,22−24] Moreover, the a axis is similar to that of the PE unit cell (a = 7.40 Å)[25] and only the b axis is slightly higher than that of PE (b = 4.93 Å), indicating that the carbonyl groups allow a perfect interdigitation of chains and a close lateral packing without significant expansion of the unit cell. This favorable packing seems to be not largely dependent on the number of methylene groups in the chains, and also in the case of an even number of methylene groups that gives a low symmetry of the chain, a close lateral packing is maintained.

CONCLUSIONS

The crystal structure of PHL has been resolved by analysis of X-ray powder diffraction profiles of the as-prepared and melt-crystallized samples and ED of single crystals. PHL has been synthesized by ROP of η-heptalactone using DPP as catalyst, and the η-heptalactone monomer has been prepared by oxidation of cycloheptanone.

Hexagonal-shaped flat PHL single crystals were obtained from a dilute solution in 1-hexanol. The ED pattern of single crystals suggests an orthorhombic unit cell with axes a = 7.36 Å and b = 5.04 Å. The ED pattern shows the same main reflections found in the X-ray powder diffraction profiles of as-prepared and melt-crystallized samples, indicating that PHL crystallizes in the identical crystalline form by crystallization from dilute or polymerization solution and from the melt.

A low-energy *trans* planar conformation of PHL with a chain period equal to c = 10.07 Å has been proposed.

The complete crystal structure has been resolved from the X-ray diffraction and ED data and calculations of the lattice energy. The low-energy model structure has been then refined with the Rietveld powder diffraction full-profile refinement and a satisfactory agreement between experimental and calculated diffraction patterns has been achieved. In the proposed final refined model, chains of PHL in *trans* planar conformations are packed in the orthorhombic unit cell with axes a = 7.37 Å, b = 5.05 Å, and c = 10.07 Å according to the monoclinic space group $P2_1$ (unique axis b) but keeping the orthorhombic symmetry of the unit cell with β = 90°. Two antiparallel polymer chains are hosted in the unit cell and the carbon atom of the carbonyl group of one chain is shifted along c by 0.159c with respect to the carbonyl group of the other antiparallel chain.

ASSOCIATED CONTENT

Supporting Information

The Supporting Information is available free of charge at https://pubs.acs.org/doi/10.1021/acs.macromol.3c00710.

Experimental details of synthesis and molecular and structural characterization by ^{1}H NMR, ^{13}C NMR, SEC, X-ray diffraction, and DSC; ^{1}H NMR and ^{13}C NMR spectra, and SEC curve of the synthesized sample of PHL; details of the preparation of single crystals, structure factors calculations, and crystal structure refinement (PDF)

AUTHOR INFORMATION

Corresponding Authors

Anna Malafronte − *Dipartimento di Scienze Chimiche, Università degli Studi di Napoli Federico II, I-80126 Napoli, Italy;* orcid.org/0000-0002-7854-5823; Email: anna.malafronte@unina.it

Claudio De Rosa − *Dipartimento di Scienze Chimiche, Università degli Studi di Napoli Federico II, I-80126 Napoli, Italy;* orcid.org/0000-0002-5375-7475; Email: claudio.derosa@unina.it

Authors

Miriam Scoti − *Dipartimento di Scienze Chimiche, Università degli Studi di Napoli Federico II, I-80126 Napoli, Italy;* orcid.org/0000-0001-9225-1509

Maria Rosaria Caputo − *POLYMAT and Department of Polymers and Advanced Materials, Physics, Chemistry and Technology, Faculty of Chemistry, University of the Basque Country UPV/EHU, 20018 Donostia-San Sebastián, Spain*

Bo Li − *University of Birmingham, Birmingham B152TT, U.K.*

Rachel K. O' Reilly − *University of Birmingham, Birmingham B152TT, U.K.;* orcid.org/0000-0002-1043-7172

Andrew P. Dove − *University of Birmingham, Birmingham B152TT, U.K.;* orcid.org/0000-0001-8208-9309

Alejandro J. Müller − *POLYMAT and Department of Polymers and Advanced Materials, Physics, Chemistry and Technology, Faculty of Chemistry, University of the Basque Country UPV/EHU, 20018 Donostia-San Sebastián, Spain; IKERBASQUE, Basque Foundation for Science, 48009 Bilbao, Spain;* orcid.org/0000-0001-7009-7715

Complete contact information is available at: https://pubs.acs.org/10.1021/acs.macromol.3c00710

Notes

The authors declare no competing financial interest.

ACKNOWLEDGMENTS

The task force "Polymers and Biopolymers" of the University of Napoli Federico II is acknowledged. Financial support from

project 3A-Italy, MICS−PNRR MUR − M4C2 - I 1.3 (PE00000004) is gratefully acknowledged. A.J.M. acknowledges funding from the Basque Government through grant IT1503-22.

REFERENCES

(1) Siddique, R.; Khatib, J.; Kaur, I. Use of Recycled Plastic in Concrete: A Review. *Waste Manage.* **2008**, *28*, 1835−1852.
(2) Rosenboom, J. G.; Langer, R.; Traverso, G. Bioplastics for a circular economy. *Nat. Rev. Mater.* **2022**, *7*, 117−137.
(3) Huang, J.-C.; Shetty, A. S.; Wang, M.-S. Biodegradable plastics: A review. *Adv. Polym. Technol.* **1990**, *10*, 23−30.
(4) RameshKumar, S.; Shaiju, P.; O'Connor, K. E.; Ramesh Babu, P. Bio-Based and Biodegradable Polymers-State-of-the-Art, Challenges and Emerging Trends. *Curr. Opin. Green Sustain. Chem.* **2020**, *21*, 75−81.
(5) *Degradable Aliphatic Polyesters*, Advances in Polymer Science, (POLYMER, volume 157), Albertsson, A.-C., Ed.; Springer: Berlin, Heidelberg, 2002.
(6) Naira, L. S.; Laurencina, C. T. Biodegradable polymers as biomaterials. *Prog. Polym. Sci.* **2007**, *32*, 762−798.
(7) Ulery, B. D.; Nair, L. S.; Laurencin, C. T. Biomedical Applications of Biodegradable Polymers. *J. Polym. Sci., Part B: Polym. Phys.* **2011**, *49*, 832−864.
(8) Chatani, Y.; Suehiro, K.; Okita, Y.; Tadokoro, H.; Chujo, K. Structural Studies of Polyesters. I Crystal Structure of Polyglycolide. *Die Makromol. Chem.* **1968**, *113*, 215−229.
(9) Kim, E.; Uyama, H.; Doi, Y.; Ha, C.-S.; Iwata, T. Crystal Structure and Morphology of Poly(11-undecalactone) Solution-Grown Single Crystals. *Macromolecules* **2004**, *37*, 7258−7264.
(10) Suehiro, K.; Chatani, Y.; Tadokoro, H. Structural Studies of Polyesters. VI. Disordered Crystal Structure (Form II) of Poly(β-propiolactone). *Polym. J.* **1975**, *7*, 352−358.
(11) Furuhashi, Y.; Iwata, T.; Sikorski, P.; Atkins, E.; Doi, Y. Structure and Morphology of the Aliphatic Polyester Poly-β-propiolactone in Solution-Grown Chain-Folded Lamellar Crystals. *Macromolecules* **2000**, *33*, 9423−9431.
(12) Su, F.; Iwata, T.; Tanaka, F.; Doi, Y. Crystal Structure and Enzymatic Degradation of Poly(4-hydroxybutyrate). *Macromolecules* **2003**, *36*, 6401−6409.
(13) Pazur, R. J.; Raymond, S.; Hocking, P. J.; Marchessault, R. H. Molecular modelling of helical and extended-chain polyhydroxybutyrates and polytetramethylene succinate. *Polymer* **1998**, *39*, 3065−3072.
(14) Nakamura, K.; Yoshie, N.; Sakurai, M.; Inoue, Y. A structural study of the crystalline state of the bacterial copolyester poly (3-hydroxybutyrate-co-4-hydroxybutyrate). *Polymer* **1994**, *35*, 193−197.
(15) Su, F.; Iwata, T.; Sudesh, K.; Doi, Y. Electron and X-ray diffraction study on poly(4-hydroxybutyrate). *Polymer* **2001**, *42*, 8915−8918.
(16) Furuhashi, Y.; Sikorski, P.; Atkins, E.; Iwata, T.; Doi, Y. Structure and morphology of the aliphatic polyester poly(δ-valerolactone) in solution-grown, chain-folded lamellar crystals. *J. Polym. Sci., Part B: Polym. Phys.* **2001**, *39*, 2622−2634.
(17) Bittiger, H.; Marchessault, R. H. Crystal structure of poly-ε-caprolactone. *Acta Crystallogr.* **1970**, *B26*, 1923−1927.
(18) Chatani, Y.; Okita, Y.; Tadokoro, H.; Yamashita, Y. Structural Studies of Polyesters. III. Crystal Structure of Poly-ε-caprolactone. *Polym. J.* **1970**, *1*, 555−562.
(19) Hu, H.; Dorset, D. L. Crystal Structure of Poly-ε-caprolactone. *Macromolecules* **1990**, *23*, 4604−4607.
(20) Dorset, D. L. Electron crystallography of linear polymers: direct structure analysis of poly(epsilon-carprolactone). *Proc. Natl. Acad. Sci. U. S. A.* **1991**, *88*, 5499−5502.
(21) Dorset, D. L. Direct determination of polymer crystal structures from fibre and powder X-ray data. *Polymer* **1997**, *38*, 247−253.
(22) Kim, E.; Uyama, H.; Doi, Y.; Ha, C.-S.; Iwata, T. Crystal structure and morphology of poly(16-hexadecalactone) chain-folded lamellar crystals. *Macromol. Biosci.* **2005**, *5*, 734−742.
(23) Kim, E.; Uyama, H.; Doi, Y.; Ha, C.-S.; Iwata, T. Crystal Structure and Morphology of Poly(12-dodecalactone). *Biomacromolecules* **2005**, *6*, 572−579.
(24) Gazzano, M.; Malta, V.; Focarete, M. L.; Scandola, M.; Gross, R. A. Crystal structure of poly(ω-pentadecalactone). *J. Polym. Sci., Part B: Polym. Phys.* **2003**, *41*, 1009−1013.
(25) Bunn, C. W. The crystal structure of long-chain normal paraffin hydrocarbons. The "shape" of the CH_2 group. *Trans. Faraday Soc.* **1939**, *35*, 482−491.
(26) Mohamed, R. M.; Yusoh, K. A Review on the Recent Research of Polycaprolactone (PCL). *Adv. Mater. Res.* **2016**, *1134*, 249−255.
(27) Labet, M.; Thielemans, W. Synthesis of Polycaprolactone: A Review. *Chem. Soc. Rev.* **2009**, *38*, 3484−3504.
(28) Tang, X.; Shi, C.; Zhang, Z.; Chen, E. Y. Crystalline Aliphatic Polyesters from Eight-membered Cyclic (Di) Esters. *J. Polym. Sci.* **2022**, *60*, 3478−3488.
(29) Van Der Mee, L.; Helmich, F.; De Bruijn, R.; Vekemans, J. A. J. M.; Palmans, A. R. A.; Meijer, E. W. Investigation of Lipase-Catalyzed Ring-Opening Polymerizations of Lactones with Various Ring Sizes: Kinetic Evaluation. *Macromolecules* **2006**, *39*, 5021−5027.
(30) Tang, X. Chemical Synthesis of Polyhydroxyalkanoates via Metal-Catalyzed Ring-Opening Polymerization of Cyclic Esters. *Advances in Polymer Science*, 2022, vol *119*; pp 1−21.
(31) Shakaroun, R. M.; Dhaini, A.; Ligny, R.; Alaaeddine, A.; Guillaume, S. M.; Carpentier, J. F. Stereo-electronic contributions in yttriummediated stereoselective ring-opening polymerization of functional racemic β-lactones: ROP of 4-alkoxymethylene-β-propiolactones with . bulky exocyclic chains. *Polym. Chem.* **2023**, *14*, 720−727.
(32) Tang, X.; Chen, E. Y.-X. Toward Infinitely Recyclable Plastics Derived from Renewable Cyclic Esters. *Chem* **2019**, *5*, 284−312.
(33) Carpentier, J.-F. Rare-earth complexes supported by tripodal tetradentate bis(phenolate) ligands: a privileged class of catalysts for ring-opening polymerization of cyclic esters. *Organometallics* **2015**, *34*, 4175−4189.
(34) Carpentier, J.-F. Discrete Metal Catalysts for Stereoselective Ring-Opening Polymerization of Chiral Racemic β-Lactones. *Macromol. Rapid Commun.* **2010**, *31*, 1696−1705.
(35) Thomas, C. M. Stereocontrolled ring-opening polymerization of cyclic esters: synthesis of new polyester microstructures. *Chem. Soc. Rev.* **2010**, *39*, 165−173.
(36) Dechy-Cabaret, O.; Martin-Vaca, B.; Bourissou, D. Controlled Ring-Opening Polymerization of Lactide and Glycolide. *Chem. Rev.* **2004**, *104*, 6147−6176.
(37) Okada, M. Chemical syntheses of biodegradable polymers. *Prog. Polym. Sci.* **2002**, *27*, 87−133.
(38) Kamber, N. E.; Jeong, W.; Waymouth, R. M.; Pratt, R. C.; Lohmeijer, B. G. G.; Hedrick, J. L. Organocatalytic Ring-Opening Polymerization. *Chem. Rev.* **2007**, *107*, 5813.
(39) Kiesewetter, M. K.; Shin, E. J.; Hedrick, J. L.; Waymouth, R. M. Organocatalysis: Opportunities and Challenges for Polymer Synthesis. *Macromolecules* **2010**, *43*, 2093−2107.
(40) Caputo, M. R.; Olmos, A.; Li, B.; Olmedo-Martínez, J. L.; Malafronte, A.; De Rosa, C.; Sardon, H.; O' Reilly, R. K.; Dove, A. P.; Müller, A. J. Synthesis, morphology and crystallization kinetics of Polyheptalactone (PHL) . *Biomacromolecules* **2023**, submitted.
(41) Arno, M. C.; Inam, M.; Coe, Z.; Cambridge, G.; Macdougall, L. J.; Keogh, R.; Dove, A. P.; O'Reilly, R. K. Precision Epitaxy for Aqueous 1D and 2D Poly (ε-Caprolactone) Assemblies. *J. Am. Chem. Soc.* **2017**, *139*, 16980−16985.
(42) Ottou, W. N.; Sardon, H.; Mecerreyes, D.; Vignolle, J.; Taton, D. Update and Challenges in Organo-Mediated Polymerization Reactions. *Prog. Polym. Sci.* **2016**, *56*, 64−115.
(43) Dauber-Osguthorpe, P.; Roberts, V. A.; Osguthorpe, D. J.; Wolff, J.; Genest, M.; Hagler, A. T. Structure and energetics of ligand

https://doi.org/10.1021/acs.macromol.3c00710
Macromolecules 2023, 56, 4153−4162

binding to proteins: E. coli dihydrofolate reductase-trimethoprim, a drug-receptor system. *Proteins: Struct., Funct., Genet.* **1988**, *4*, 31−47.
(44) Rietveld, H. M. A profile refinement method for nuclear and magnetic structures. *J. Appl. Crystallogr.* **1969**, *2*, 65−71.
(45) Young, R. A. *The Rietveld Method, IUCr Monographies of Crystallography, 5*; Oxford University Press: Oxford, 1993.
(46) Iwata, T.; Doi, Y. Morphology and enzymatic degradation of poly(ε-caprolactone) single crystals: does a polymer single crystal consist of micro-crystals? *Polym. Int.* **2002**, *51*, 852−858.

https://doi.org/10.1021/acs.macromol.3c00710
Macromolecules 2023, 56, 4153−4162